

ORIGINAL ARTICLE

Water-soluble dietary fiber alleviates cancer-induced muscle wasting through changes in gut microenvironment in mice

Tomoki Sakakida¹  | Takeshi Ishikawa¹  | Toshifumi Doi¹ | Ryuichi Morita¹ | Yuki Endo¹  | Shinya Matsumura¹ | Takayuki Ota¹ | Juichiro Yoshida¹ | Yasuko Hirai² | Katsura Mizushima² | Yasuki Higashimura³ | Ken Inoue¹ | Tetsuya Okayama¹ | Kazuhiko Uchiyama¹ | Tomohisa Takagi¹ | Aya Abe⁴ | Ryo Inoue⁵ | Yoshito Itoh¹ | Yuji Naito²

¹Department of Molecular Gastroenterology and Hepatology, Kyoto Prefectural University of Medicine, Kyoto, Japan

²Department of Human Immunology and Nutrition Science, Kyoto Prefectural University of Medicine, Kyoto, Japan

³Department of Food Science, Ishikawa Prefectural University, Nonoichi, Japan

⁴Nutrition Division, Taiyo Kagaku Co. Ltd., Yokkaichi, Japan

⁵Laboratory of Animal Science, Department of Applied Biological Sciences, Faculty of Agriculture, Setsunan University, Hirakata, Japan

Correspondence

Takeshi Ishikawa, Kyoto Prefectural University of Medicine, 465 Kajicho, Hirokoji agaru, Kawaramachi Street, Kamigyoku, Kyoto city, Kyoto 602-8566, Japan.

Email: iskw-t@koto.kpu-m.ac.jp

Funding information

MAFF Commissioned project study on "Project for the realization of foods and dietary habits to extend healthy life expectancy" (Grant/Award Number: JPJ009842); JSPS KAKENHI (Grant/Award Number: JP 20K07787)

Abstract

Cancer cachexia and the associated skeletal muscle wasting are considered poor prognostic factors, although effective treatment has not yet been established. Recent studies have indicated that the pathogenesis of skeletal muscle loss may involve dysbiosis of the gut microbiota and the accompanying chronic inflammation or altered metabolism. In this study, we evaluated the possible effects of modifying the gut microenvironment with partially hydrolyzed guar gum (PHGG), a soluble dietary fiber, on cancer-related muscle wasting and its mechanism using a colon-26 murine cachexia model. Compared with a fiber-free (FF) diet, PHGG contained fiber-rich (FR) diet-attenuated skeletal muscle loss in cachectic mice by suppressing the elevation of the major muscle-specific ubiquitin ligases Atrogin-1 and MuRF1, as well as the autophagy markers LC3 and Bnip3. Although tight-junction markers were partially reduced in both FR and FF diet-fed cachectic mice, the abundance of *Bifidobacterium*, *Akkermansia*, and unclassified *S24-7 family* increased by FR diet, contributing to the retention of the colonic mucus layer. The reinforcement of the gut barrier function resulted in the controlled entry of pathogens into the host system and reduced circulating levels of lipopolysaccharide-binding protein (LBP) and IL-6, which in turn led to the suppression of proteolysis by downregulating the ubiquitin-proteasome system and autophagy pathway. These results suggest that dietary fiber may have the potential to alleviate skeletal muscle loss in cancer cachexia, providing new insights for developing effective strategies in the future.

Abbreviations: ASV, amplicon sequence variant; BP, biological process; C26, colon-26; CC, cellular component; CT, control; DEG, differentially expressed gene; FF, fiber-free; FR, fiber-rich; G-CSF, granulocyte-colony-stimulating factor; GM-CSF, granulocyte-monocyte-colony-stimulating factor; JAM, junctional adhesion molecule; KC, keratinocyte chemoattractant; MAFbx, muscle atrophy F-box; MCP-1, monocyte chemoattractant protein-1; MF, molecular function; MIP-1a, macrophage inflammatory protein-1a; Muc2, mucin2; MuRF1, muscle RING finger 1; MyHC, myosin heavy chain; OTU, operational taxonomic unit; PHGG, partially hydrolyzed guar gum; SCFA, short-chain fatty acid; TJP, tight-junction protein; ZO-1, zonula occludens-1.

This is an open access article under the terms of the [Creative Commons Attribution-NonCommercial](https://creativecommons.org/licenses/by-nc/4.0/) License, which permits use, distribution and reproduction in any medium, provided the original work is properly cited and is not used for commercial purposes.

© 2022 The Authors. *Cancer Science* published by John Wiley & Sons Australia, Ltd on behalf of Japanese Cancer Association.

KEYWORDS

cachexia, dietary fiber, gut microbiome, prebiotics, sarcopenia

1 | INTRODUCTION

Cancer cachexia is a complex metabolic disorder characterized by severe wasting of skeletal muscle and adipose tissue, loss of physical function, and anorexia. Sarcopenia, defined as reductions in the muscle mass, strength, and physical condition, is also an important disorder in cancer patients. Severe cachexia and sarcopenia are associated with high mortality, reduced quality of life, and poor outcomes of anticancer treatments, contributing to at least 20% of cancer deaths.¹ Cachexia is driven by inflammation; however, because of its multifactorial nature, the pathogenesis is still incompletely understood.

In catabolic conditions such as cancer, muscle wasting is induced by the continuous imbalance between protein synthesis and degradation.² Increased protein degradation is considered to be the main cause, supported by the fact that skeletal muscle mass cannot be restored by amino acid supplementation alone.³ Previous reports demonstrated that atrogin-1/muscle atrophy F-box (MAFbx) and muscle RING finger 1 (MuRF1), the two ubiquitin ligases of the ubiquitin-proteasome pathway, play a major role in muscle proteolysis as part of cancer-related muscle wasting.^{4,5} Recently, the autophagy/lysosomal pathway has also been regarded as important.^{3,6} These pathways are mediated by procachectic cytokines such as IL-6, TNF- α , and IFN- γ and other regulators.⁷ In particular, IL-6 is regarded as the key mediator for the progression of cachexia, with its levels associated with patients' longevity.⁸

Recently, researchers have focused on the crosstalk between gut microbiota and the pathophysiology of age-related sarcopenia, the so-called "gut-muscle axis."^{9,10} Moreover, gut barrier dysfunction has been demonstrated in several murine cachectic models, suggesting the relevance of gut microbiota to muscle metabolism during cancer.^{11,12} Although a few studies on cachexia focusing on interventions to the gut environment have been reported,¹³⁻¹⁵ limited evidence is available.

Dietary fiber, a nondigestible nutrient including polysaccharides, is drawing attention. The gut microbiome ferments dietary polysaccharides into short-chain fatty acids (SCFAs), absorbable substances that act as mediators of favorable metabolic activities in the host.¹⁶ Recent studies reported that SCFAs partly mediate skeletal muscle metabolism and function in aging or obese mice;^{17,18} however, their role in cancer-associated muscle metabolism remains unclear.

Partially hydrolyzed guar gum (PHGG), a water-soluble dietary fiber derived from guar seeds, is known for its high fermentability and stimulation of SCFA production.¹⁹ Therefore, PHGG is regarded as one of the most beneficial dietary fibers and considered a functional food.

Based on these studies, we hypothesized that PHGG intake would exert a systemic anti-inflammatory effect through changes in

the intestinal environment and barrier function, thereby suppressing muscle atrophy in cancer cachexia. We used a well-established colon-26 (C26) cachexia model and evaluated the characteristics and mechanisms.

2 | MATERIALS AND METHODS

2.1 | Cell culture and treatments

The colon-26 murine adenocarcinoma cell line was obtained from Cosmo Bio Co., Ltd and was maintained in RPMI-1640 medium supplemented with 10% FBS and penicillin (100 IU/ml)/streptomycin (100 μ g/ml) in a humidified 5% CO₂ incubator at 37°C. C2C12 myoblasts were obtained from KAC Co., Ltd and were cultured in DMEM containing 10% FBS and penicillin/streptomycin. When myoblasts reached approximately 90% confluence, the medium was replaced with DMEM containing 2% horse serum with medium changes every 2 days for differentiation into myotubes. After 96 hours, the myotubes were treated with a 10-mM concentration of SCFA cocktail (acetate/propionate/butyrate ratio = 60:25:15, by the molar ratio in plasma) for 24 hours, followed by stimulation with 1 μ g/ml of LPS for 2 hours, based on previous studies.^{20,21}

2.2 | Animals and diet

Male BALB/c mice (6 weeks old, Shimizu Laboratory Supplies) were caged individually in a room with a temperature of 18-24°C, humidity of 40%-70%, and a 12-hour light/dark cycle. Two types of diet were prepared: a fiber-rich (FR) diet (cellulose-removed AIN-93G diet < Research Diet, Nihon Clea, Tokyo, Japan > supplemented with 5% PHGG), and fiber-free (FF) diet (cellulose-removed AIN-93G diet). The detailed components of diets are described in Table S1.

2.3 | Experimental design

The C26 cachexia model was designed by injecting 5×10^6 cells in 0.2 ml of saline subcutaneously into the right flank of mice anesthetized by isoflurane inhalation, as previously reported.²² After one week of acclimatization, they were randomly assigned to four groups according to their body weight and fed the FR or FF diet for 2 weeks. Next, on day 0, either C26 cells or a saline solution was injected subcutaneously. Thus, the experiment comprised the following four groups: C26-FR, C26-FF groups (C26 cell-transplanted mice fed FR or FF diet) and CT-FR, CT-FF groups (sham-injected mice fed FR or FF diet). Two independent experiments in which mice were

sacrificed on days 9 and 21 were performed to estimate the mechanisms underlying early and late phases of cachexia. The body weight, food intake, and tumor growth were recorded every other day. The tumor size was calculated as $a \times b^2/2$, with a the maximal and b the minimal diameter of the tumor.

For the first experiment, on day 21, mice ($n = 7$ or 8 per group) were adequately anesthetized with isoflurane gas and blood was collected by heart puncture, centrifuged³ at $500 \times g$ for 5 minutes, and the plasma was stored at -80°C . The gastrocnemius muscle, fecal-containing cecum, colon, terminal ileum, and tumor were harvested, weighed, and stored at -80°C . The colon was immediately preserved in Carnoy's solution for 3 hours and then transferred to fresh methanol until further use. For the second experiment, we performed the same protocols as above ($n = 8$ mice in the C26-FR, C26-FF groups and $n = 5$ mice in the CT-FR, CT-FF groups), sacrificing mice and collecting the sections as described above on day 9.

2.4 | Assays for circulating cytokines and lipopolysaccharide-binding protein (LBP)

The cytokines in plasma samples on day 21 (IL-1 α , IL-1 β , IL-2, IL-3, IL-4, IL-5, IL-6, IL-9, IL-10, IL-12[p40], IL-12[p70], IL-13, IL-17A, IFN- γ , TNF- α , eotaxin, granulocyte-colony-stimulating factor [G-CSF], granulocyte-monocyte-colony-stimulating factor [GM-CSF], keratinocyte chemoattractant [KC], monocyte chemoattractant protein-1 [MCP-1], macrophage inflammatory protein [MIP]-1a, MIP-1b, and RANTES) were measured with a Bio-Plex multiplex assay system (Bio-Rad) following the manufacturer's instructions. Circulating levels of IL-6 on day 9 and LBP on day 9 and 21 were measured using ELISA kits (Hycult Biotech and R&D Systems, Inc.) according to the manufacturer's instructions.

2.5 | Tissue and cell mRNA analyses

Total RNA was extracted and then reverse-transcribed into complementary DNA. Polymerase chain reaction (PCR) was conducted by the 7300 Real-Time PCR system (Applied Biosystems). Primer sequences are detailed in Table S2.

2.6 | RNA microarray analysis

Isolated RNA from the gastrocnemius muscle was subjected to microarray analysis using Affymetrix GeneChip Mouse Gene 1.0 ST Array (Thermo Fisher Scientific) according to the manufacturer's instructions ($n = 3$ per group sacrificed on day 21). Comparison of the mean differences was made between the two groups selected (C26-FF vs CT-FF group and C26-FR vs C26-FF group) using a two-tailed parametric t test. We defined differentially expressed genes (DEGs) as those with an absolute fold change ≥ 1.5 with $p < 0.05$. Next, for function annotation of DEGs, enrichment analysis based

on the Gene Ontology (GO) category database was applied using the DAVID Bioinformatics database.²³ Categories of biological process (BP), cellular component (CC), and molecular function (MF) were analyzed, and we excluded the drawn categories if the annotated genes were less than five, showed no significant difference, or the fold change was < 1.5 .²³

2.7 | FISH and immunofluorescence staining with histological analysis

Fluorescence in situ hybridization and immunofluorescence staining for Muc2 and EUB was performed using colonic sections that were fixed and paraffinized. Sections were deparaffinized and dehydrated before being mounted with the eubacterial probe EUB-338-Cy5 (Sigma-Aldrich), which targets nearly all bacteria, for hybridization, and primary antibody staining was performed by covering the sections with 1:100 diluted rabbit anti-Muc2 antibodies (Santa Cruz Biotechnology) at 4°C overnight. For secondary antibody staining, the sections were covered by a 1:1,000 dilution of goat anti-rabbit IgG antibody conjugated with Alexa Fluor 594 (Abcam) and Phalloidin-iFluor 488 (Abcam) and incubated at room temperature for 2 hours. These were visualized using an Olympus FV10i confocal laser scanning microscope (Olympus). The colonic mucus layer thickness was measured using the method previously described.²⁴

C2C12 myotubes were cultured in differential medium with either LPS (1 $\mu\text{g}/\text{ml}$) or LPS and SCFA cocktail (10 mM) for 48 hours. These cells were fixed with 4% paraformaldehyde, incubated with 1:250 diluted mouse anti-myosin heavy chain (MyHC) antibody (MAB4470, R&D Systems) and 1:500 diluted Alexa Fluor 488-conjugated secondary antibody (Abcam), and visualized by fluorescence microscopy. The diameter of myotubes in ten random fields was measured using Image J software version 1.53 (National Institutes of Health), as previously reported.²¹

2.8 | Analysis of cecal bacteria

We extracted the genomic DNA of the bacteria from the collected cecal contents as reported previously.²⁵ A two-step PCR method was carried out using purified DNA samples to acquire the sequence library. First, 16S (V3-V4) Metagenomic Library Construction Kit for NGS (Takara Bio Inc.) with primers 341F (5'-TCGTCGGCAGCGTCAGATGTGTATAAGAGACAG CCTACGGGNGGCWGCAG-3') and 806R (5'-GTCTCGTGG GCTCGGAGATGTGTATAAGAGACAGGGACTACHVGGGT WTCTAAT-3') was used to amplify the V3-4 region of the 16S rRNA genes in each sample, and the amplicons were purified by AMPureXP (Beckman Coulter, Inc.). The second PCR was performed using Nextra XT Index Kit v2 (Illumina) to attach specific index sequences for each sample. With the prepared libraries, sequencing was performed at Takara Bio's Biomedical Center using the MiSeq Reagent v3 kit and MiSeq with 250 paired-end strategy.

The sequence data were analyzed using QIIME2 2020.8. The detailed quality statistics for each sample are summarized in Table S3. Assignment of taxonomy was achieved through the Sklearn classifier algorithm against the Greengenes database 13_8 (99% OTUs full-length sequences). In this study, singletons and ASVs assigned to mitochondria and chloroplasts were removed. The phylogenetic tree was generated by SATé-enabled phylogenetic placement (SEPP).²⁶ Metrics regarding alpha (Chao1 and Shannon indices) and beta diversities (UniFrac distances) were calculated by QIIME2 by setting the sampling depth at 5000 reads. Significance of β -diversity was assessed by permutational multivariate analysis of variance (PERMANOVA) using QIIME2.

2.9 | Analysis of fecal SCFAs

Approximately 30 mg of cecal contents were suspended in 0.5 ml of 14% perchloric acid for protein elimination, centrifuged at $10,000 \times g$ for 5 minutes at 4°C, and the supernatant solution was screened through a cellulose acetate membrane filter of 0.45 μm pore size. The amount of organic acids was measured by ion-exclusion high-performance liquid chromatography, as described previously.²⁷

2.10 | Statistical analyses

Results are presented as the mean \pm SEM, except for data from microbiome analysis where α -diversity and relative abundance of representative phyla and genera are presented by box-and-whisker plots with minimal and maximal values. The significance of differences was assessed using Student's *t* test or the Mann-Whitney *U* test when comparing two groups. When comparing multiple groups, one-way ANOVA followed by post hoc Tukey multiple comparison test or the Kruskal-Wallis test followed by the Steel-Dwass post hoc test was used. All statistical tests were two-sided, and $p < 0.05$ was set as the level of significance. Statistical analyses were performed using JMP® pro 15 (SAS Institute Inc.) unless otherwise stated.

3 | RESULTS

3.1 | Fiber-rich diet attenuates body weight and muscle volume in C26 murine model

The overall protocol of the experiments is shown in Figure 1A. First, we compared the body weight and muscle volume between mice fed FR and FF diets. The body weight started to decrease gradually from days 3 to 7 in the C26 groups, whereas it increased steadily in the CT groups, with a slight difference in food intake (Figure 1B,C). Body weight was maintained in the latter period in the C26-FR group, while it continuously decreased in the C26-FF group, consequently leading to large but nonsignificant differences among groups in body and carcass weights when sacrificed on day 21 (Figure 1D,E).

Importantly, C26 transplantation induced a significant loss of gastrocnemius muscle weight, but this was greater in the C26-FF group, resulting in a significant difference in the C26-FR and C26-FF groups (Figure 1F). In addition, dietary treatment did not affect the tumor size in the C26 groups, or body and gastrocnemius weights in the CT groups (Figure 1D,E,G).

3.2 | Fiber-rich diet reduces markers of skeletal muscle atrophy in cancer cachexia

To assess the mechanisms of the anticachectic effect of the FR diet, we initially measured markers related to proteolysis of gastrocnemius muscles on days 9 and 21. On day 21, the expressions of Atrogin-1 and MuRF1, key atrogenes, and LC3a and LC3b, representative autophagy markers, were elevated in the C26-FF group, whereas they were markedly reduced in the C26-FR group (Figure 2A–D). Furthermore, FoxO1, a member of the Forkhead Box O family which regulates the expression of ubiquitin ligases and autophagy genes,²⁸ also showed the same pattern (Figure 2E). Tfam, a marker of mitochondrial biogenesis, was significantly elevated, and CPT1b, an enzyme involved in fatty acid metabolism, also showed a similar trend in the C26-FR group compared with the C26-FF group; however, another mitochondrial marker, PGC1 α , did not show any differences (Figure 2F–H). By contrast, MuRF1, LC3a, and FoxO1 were significantly decreased in the C26 groups compared with the CT groups on day 9 (Figure S1).

We subsequently performed a microarray analysis of gastrocnemius muscles of mice on day 21 ($n = 3$ per group) to gain a more comprehensive understanding of the biological processes involved in the pathogenesis of muscle wasting. Figure 2I shows the results of DEGs as volcano plots when comparing the C26-FF versus CT-FF and the C26-FR versus C26-FF groups, respectively. This chart also revealed that ubiquitin ligases including MuRF1 and Atrogin-1, autophagy markers such as LC3b, Bnip3, and Cathepsin L, and their regulator FoxO3 were significantly upregulated in the C26-FF group compared with the CT-FF group, and downregulated in the C26-FR group compared with the C26-FF group. Subsequently, to determine the biological processes altered by the tumor and FR diet ingestion, we identified overlapping DEGs by comparing two groups: upregulated genes in the C26-FF versus CT-FF groups and downregulated genes in the C26-FR versus C26-FF groups (group 1), and downregulated genes in the C26-FF versus CT-FF groups and upregulated genes in the C26-FR versus C26-FF groups (group 2)(Figure 2J). Groups 1 and 2 consisted of 196 and 263 genes, respectively, and GO analysis by DAVID tools was conducted to identify the enriched categories of BP, CC, and MF. In line with the findings mentioned above, *ubiquitin-dependent protein catabolic process*, *proteasome complex*, and *negative regulation of apoptotic process* were found in group 1 (Figure 2K). Many genes were related to specific skeletal muscle components such as *sarcoplasmic reticulum* and *sarcolemma*, and the main BP categories were *collagen fibril organization*, *muscle contraction*, and *glucose metabolic process* in group 2 (Figure 2L). The top

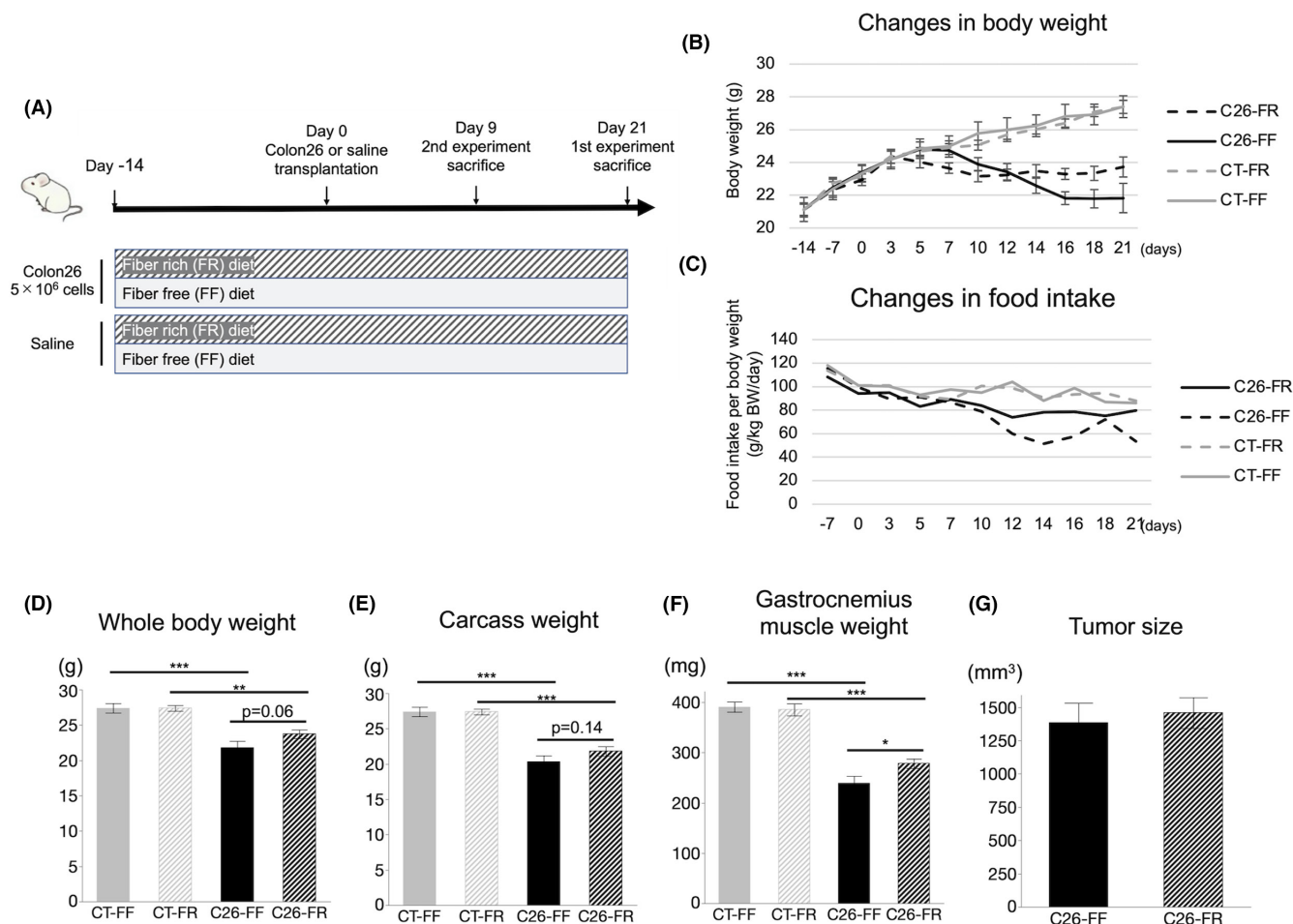


FIGURE 1 Effect of fiber-rich diet on cachectic features of colon-26 (C26) mice. A, Schematic showing the timeline of the experiment. B, C, Changes in body weight and food consumption among the CT-FF, CT-FR, C26-FF, and C26-FR groups. D-G, Whole-body weight, carcass weight, gastrocnemius-muscle weight, and tumor size on day 21. Data are shown as means \pm SEM ($n = 7$ or 8 per group). * $p < 0.05$, ** $p < 0.01$, *** $p < 0.001$. FF, fiber-free; FR, fiber-rich

30 enriched categories of DEGs in the C26-FF versus CT-FF groups and the C26-FF versus C26-FF groups are described in Tables S4–S7.

3.3 | Gut permeability markers are partially impaired in cachectic mice and do not improve with dietary fiber supplementation

Next, we investigated the intestinal environment underlying this possible beneficial effect through an expression of gut permeability markers in the colon. Mucus secretion from goblet cells and tight-junction proteins (TJPs), such as zonula occludens-1 (ZO-1), occludin, junctional adhesion molecule (JAM), and claudins, contribute to the formation of a physical barrier that protects the host from excessive gut microbiome exposure. On day 21, claudin 1,3,4, and JAM exhibited lower levels in the C26 groups (Figure 3D-G). In contrast, Muc2, ZO-1, occludin, and claudin 7 levels were higher or showed no differences in the presence of cancer (Figure 3A-C, H). These data also showed that although supplementation with dietary fiber itself increased the expression of occludin and JAM, it did not have

a definite effect on the totality. In addition, mice sacrificed on day 9 showed no significant findings regarding these parameters among the four groups (Figure S2A-H).

3.4 | Fiber deficiency reduces colonic mucus layer and promotes bacterial invasion of host

We examined the thickness of the colonic mucus layer by immunofluorescence staining of Muc2 and also validated the location of bacteria using the FISH technique. On day 9, a significantly thicker mucus layer was found in both the C26-FR and CT-FR groups (Figure 3I,K). Mucus layer measurements on day 21 revealed a thinner mucus layer in the C26 groups compared with the CT groups, although it was preserved in FR diet-fed mice and severely depleted in FF diet-fed mice, and this was accompanied by bacterial invasion into the colonic epithelium (Figure 3J,L). Lipopolysaccharide-binding protein, an acute phase response protein mainly produced by the liver, is regarded as an indicator of the antigen load of bacteria.²⁹ Notably, circulating LBP levels showed a tendency to be

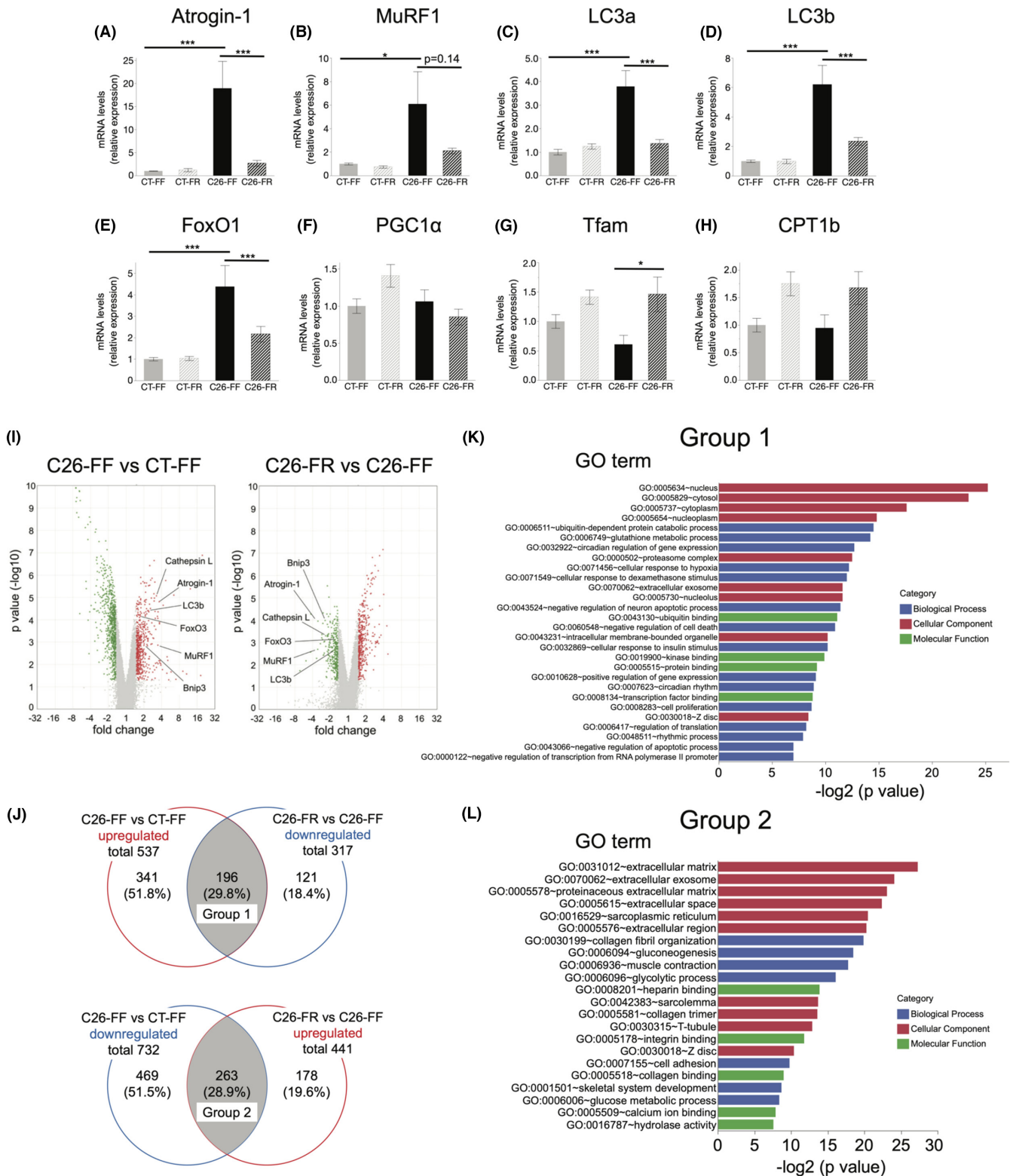


FIGURE 2 Gene expression analysis of gastrocnemius muscle. RT-PCR and microarray analysis were performed in mice on day 21. A, B, mRNA expression of the two muscle-specific ubiquitin ligases. C-E, mRNA expression of the representative autophagy markers and FoxO1. F-H, mRNA expression of the representative mitochondrial markers. I, Volcano plots from microarray analysis comparing the C26-FF versus CT-FF groups (left) and the C26-FR versus C26-FF groups (right). Red and green plots indicate genes that were up- and downregulated, respectively. J, Venn diagrams showing the number of differentially expressed genes in the C26-FF versus CT-FF groups and the C26-FR versus C26-FF groups, and the number of genes which overlap between them (defined as groups 1 and 2, respectively). K, L, Gene ontology analysis showing the enriched terms of groups 1 and 2. A-H are shown as means \pm SEM ($n = 7, 8$ per group). Microarray data (I-K) consist of $n = 3$ per group. * $p < 0.05$, ** $p < 0.01$, *** $p < 0.001$. FF, fiber-free; FR, fiber-rich

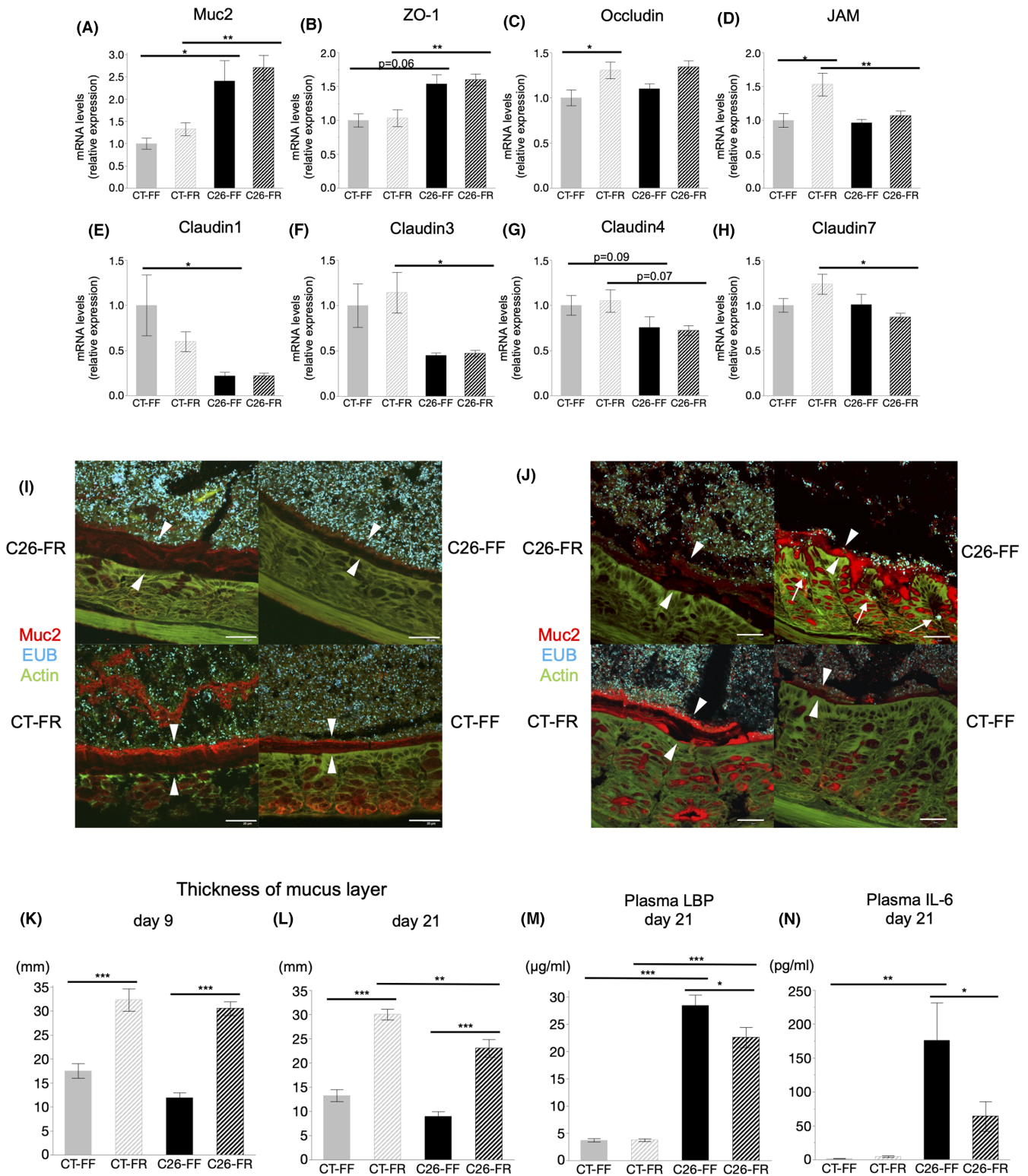


FIGURE 3 Analysis of gut barrier function and bacterial translocation. A-H, mRNA expression of markers involved in the gut barrier function on day 21. I, J, Images of the colonic sections of the C26-FR, C26-FF, CT-FR, and CT-FF groups from combined FISH and immunofluorescence staining with anti-Muc2 antibody, EUB, and phalloidin on days 9 and 21, respectively. The white arrows show the bacteria invading the host's epithelium and the white arrowheads show the mucus layers. Scale bars: 30 μm. K, L, The thickness of mucus layers among the four groups on days 9 and 21. M, N, Plasma lipopolysaccharide-binding protein (LBP) and IL-6 levels on day 21. Data are shown as means ± SEM. ($n = 7$ or 8 per group) * $p < 0.05$, ** $p < 0.01$, *** $p < 0.001$. FF, fiber-free; FR, fiber-rich

higher on day 9 (Figure S2J) and were significantly higher on day 21 (Figure 3M) in the C26-FF group compared with the C26-FR group, indicating greater bacterial susceptibility with a thinner mucus layer in cachectic mice fed the FF diet.

3.5 | Circulating IL-6 levels are elevated in C26 cachexia models but are markedly suppressed by dietary fiber consumption (plasma cytokine profile)

To elucidate the behavior of cytokines involved and the extent of systemic inflammation in the present study, we performed a comprehensive analysis of inflammatory cytokines among the four groups on day 21. Most importantly, IL-6, the key cytokine inducing cachexia, was elevated in the C26 groups, although it was markedly downregulated in the C26-FR group on both days 9 and 21 (Figure S2K, Figure 3N). Moreover, plasma levels of IL-6 and the abovementioned LBP were significantly correlated (Figure S2L). IL-5, IL-12 (p70), and MIP-1a were significantly lower in the C26 groups compared with the CT groups. IL-1a, G-CSF, and MIP-1b were lower in the C26-FR group compared with the CT-FR group, and IL-2 and GM-CSF showed lower levels in the C26-FF group compared with the CT-FF group. Of note, other cytokines known to be associated with cachexia or muscle wasting, such as TNF- α , IFN- γ , and IL-1 β , remained significantly unchanged in the presence of cancer (Figure S3).

3.6 | Fiber-rich diet alters composition of gut microbiome in cachexia models

To elucidate the gut environment underlying this model, we analyzed the microbial diversity and populations using cecal contents of mice on day 9. The C26-FR group showed reduced Chao1 and Shannon indices in microbial α -diversity compared with the C26-FF group (Figure 4A). The β -diversity of the four groups was evaluated using the weighted and unweighted UniFrac distance and visualized by principal coordinate analysis (PCoA). This demonstrated significant microbial structural differences among these groups based on both the weighted and unweighted UniFrac distance (PERMANOVA $p = 0.0001$, Figure 4B). Next, we focused our analysis on microbial abundance at different taxonomic levels. At the phylum level, a marked shift from Firmicutes to Bacteroidetes was observed with fiber supplementation in the C26 groups, resulting in a significant decrease of the Firmicutes/Bacteroidetes (F/B) ratio in the C26-FR group. Moreover, the relative abundance of Proteobacteria decreased in both the CT-FR and C26-FR groups compared with the CT-FF and C26-FF groups (Figure 4C–G). At the genus level, abundances of *Bifidobacterium*, *Akkermansia*, and unclassified S24-7 were significantly lower in the C26-FF group, although these were all restored by the FR diet. In addition, an increased abundance of *Oscillospira* was found in the C26-FF group (Figure 4H–L). Overall data at the genus level are shown in Table S8.

3.7 | Analysis of fecal short-chain fatty acids and their effects on LPS-induced C2C12 myotube atrophy

The next step was to examine SCFAs in cecal contents among the four groups on day 9. Between the CT groups, the principal metabolites, acetate, propionate, and succinate, showed significantly higher levels in mice fed the FR diet. Although the C26 groups showed relatively lower SCFA levels, the same trend as described above was found, resulting in overarching preservation in the C26-FR groups (Figure 5A–E). The results for other SCFAs are presented in Figure S4. To explore the effects of SCFAs on skeletal muscle mass, we used a well-established in vitro myotube culture model. Exposure of C2C12 myotubes to LPS induced a significant decrease in the diameter, but this was reversed on administering a cocktail of SCFAs (Figure 5F,G). The increased expression of Atrogin-1 by LPS was significantly reduced when LPS-stimulated myotubes were subjected to SCFA treatment (Figure 5H). On the other hand, MuRF1 did not show any difference (Figure 5I). We also demonstrated that the SCFA cocktail upregulated the expression of PGC1 α and Tfam but not CPT1b in C2C12 myotubes with or without LPS exposure (Figure 5J–L).

4 | DISCUSSION

Herein, we demonstrated that a PHGG-containing FR diet ameliorated muscle wasting under cancer-cachectic conditions by reinforcing the gut barrier function through alterations in the gut microbiota and subsequent anti-inflammatory effects. Consistent with previous reports,^{11,12} we showed that the gut barrier function of cachectic mice was disrupted. However, a significantly thicker colonic mucus layer was retained in mice receiving PHGG supplementation, compensating for this impairment. To our best knowledge, this is the first report to show that dietary fiber preserves the colonic mucus layer during cancer cachexia. The reinforcement of the mucus layer consequently reduced the translocation of pathogens into the host system and led to lower circulating levels of LBP and IL-6, which contributed to the suppression of proteolysis by downregulating the core factors, ubiquitin-proteasome system, and autophagy pathway.

Clinical approaches targeting the anabolic pathway have emerged sporadically, although there are very few challenges to control hypercatabolism in cancer cachexia. Therefore, it is noteworthy that suppression of the catabolic pathway was sufficient to achieve significant improvements in skeletal muscle mass and body weight. Microarray analysis offered us wider insights, showing that the genes upregulated by FR diet intake, which were depressed in response to C26, were related to the extracellular matrix and sarcolemma with enriched processes of muscle contraction and collagen fibril organization, and these all play essential roles in muscle structural integrity and function.³⁰ This suggests that a FR diet could improve not only the volume but also functional aspects of skeletal muscle.

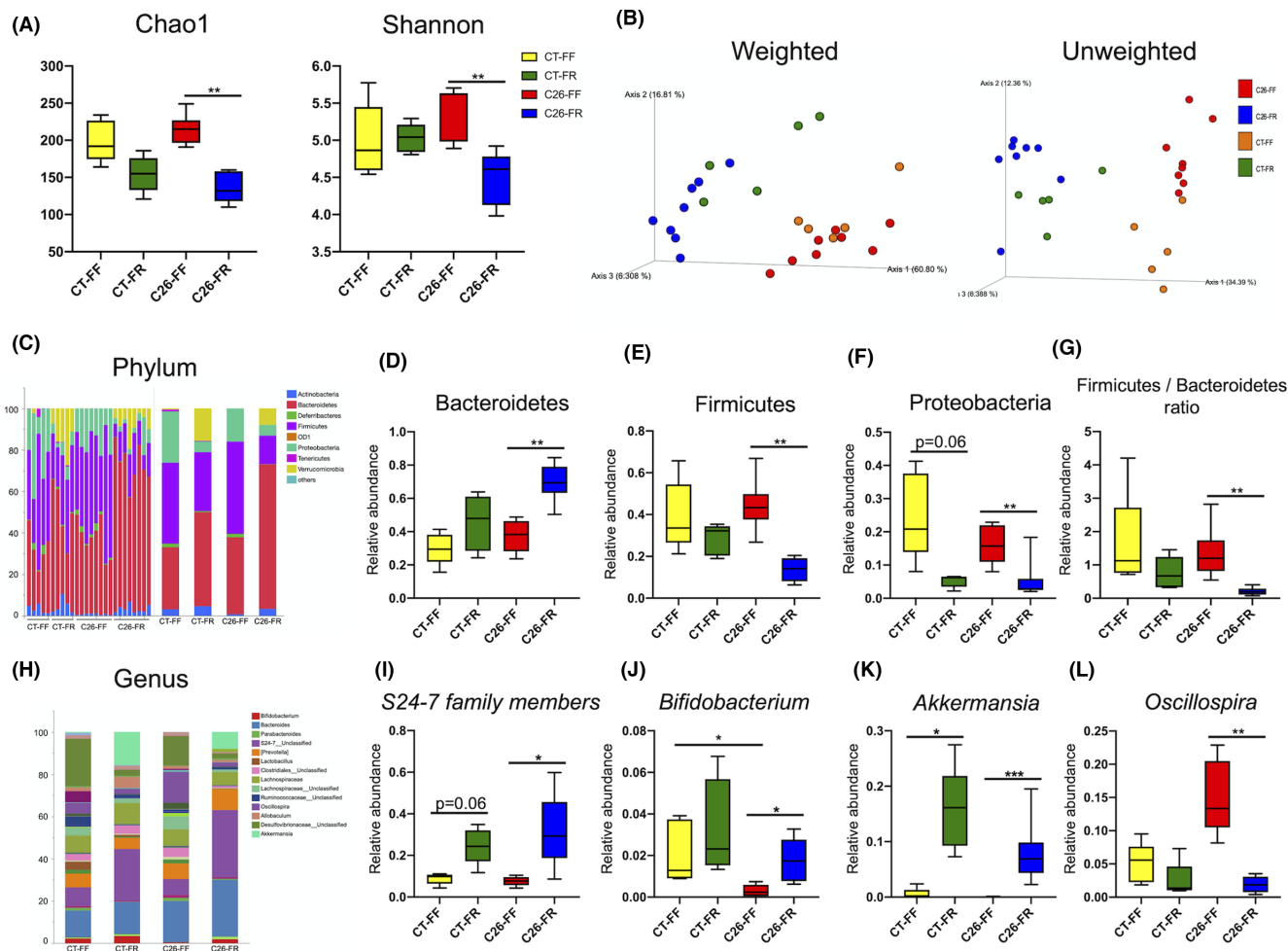


FIGURE 4 Gut microbiome composition in cecal content. The relative abundance of microbial taxa was determined by 16S rRNA analysis in mice on day 9 ($n = 8$ for the C26-FF, C26-FR groups; $n = 5$ for the CT-FF, CT-FR groups). A, α -diversity indexes of the cecal microbial community in the CT-FF, CT-FR, C26-FF, C26-FR groups. B, β -diversity is described by a principal coordinate analysis (PCoA) plot of unweighted and weighted UniFrac data. C, H, Relative abundance of microbial taxa at the phylum and genus level. D-G, Relative abundance of Bacteroidetes, Firmicutes, and Proteobacteria and the Firmicutes/Bacteroidetes ratio among the four groups. I-L, Relative abundance of S24-7 family members, *Bifidobacterium*, *Akkermansia*, and *Oscillospira*. Data are presented as whisker plots with minimal and maximal values. * $p < 0.05$, ** $p < 0.01$, *** $p < 0.001$. FF, fiber-free; FR, fiber-rich

The role of gut microbiota in cancer cachexia is receiving increasing attention, with evidence that altered intestinal homeostasis with increased gut permeability was present in conjunction with increased proinflammatory cytokines and cachectic conditions in mouse models.¹¹⁻¹³ These studies support the idea that a decrease in TJPs and degradation of the mucus layers increase gut permeability, facilitating greater absorption and translocation of bacteria or bacterial components into the circulation, contributing to systemic inflammation and ultimately cancer cachexia. Interestingly, Cani et al. previously reported a similar theory in the pathogenesis of obesity and diabetes.³¹ In our study, consistent with previous reports, we showed that expression of the colonic tight-junction markers was partially reduced in the late phase of cachexia. More importantly, the colonic mucus layer was retained throughout the course of cachexia in mice receiving PHGG, but not in the FF diet-fed mice. This result was in line with recent reports that low-fiber diets deplete the colonic mucus layer and increase permeability, resulting in systemic

chronic inflammation.^{24,32,33} Lipopolysaccharide-binding protein has been reported as a perspicuous marker of bacterial translocation in human and mouse studies.^{12,34} Circulating LBP and IL-6 showed inverse associations with the abundance of mucus in the current study. Therefore, we consider that modification of the colonic mucus barrier was a major contributor to the alleviation of systemic inflammation and subsequent anticachectic effects.

Our results of 16S rRNA analysis of cecal contents confirmed the importance of dietary fiber in maintaining gut barrier function. PCoA of β -diversity facilitated a clear distinction among the four groups in our study, indicating that gut dysbiosis occurred in response to the tumor burden, and that the microbial composition was markedly altered by PHGG supplementation. The marked shift from Firmicutes to Bacteroidetes and the decrease of Proteobacteria in the C26-FR group were the most notable change in the phylum level. These findings are of interest because similar results have been reported in the presence of

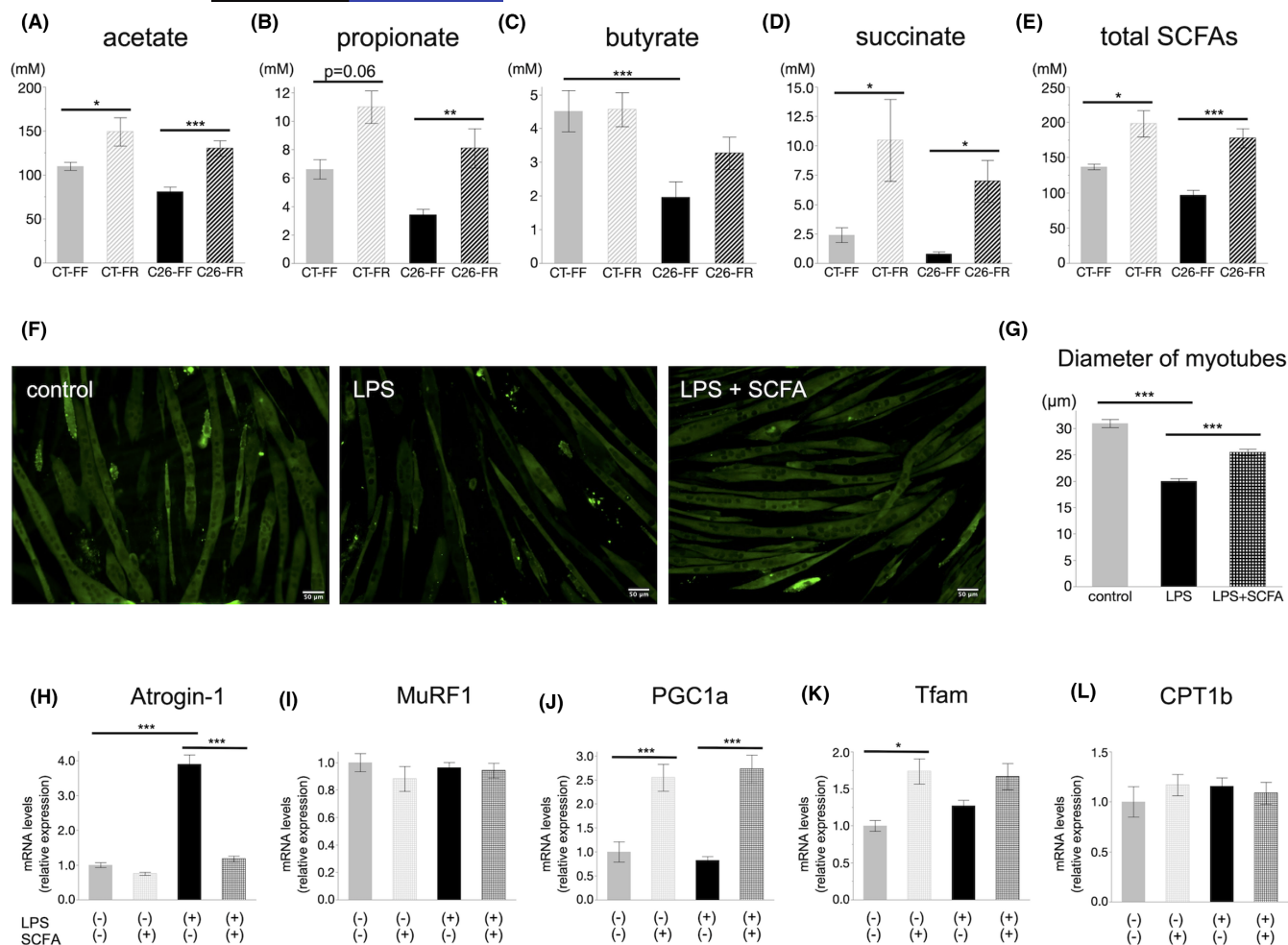


FIGURE 5 Short-chain fatty acid (SCFA) analysis in mice and effects of SCFAs on C2C12 mouse myotubes in vitro. A-E, Cecal SCFA profile in mice on day 9 among the CT-FF, CT-FR, C26-FF, and C26-FR groups ($n = 8$ for the C26-FF, C26-FR groups; $n = 5$ for the CT-FF, CT-FR groups). F, Images of immunofluorescence staining with myosin heavy chain (MyHC) in C2C12 myotubes treated with lipopolysaccharide-binding protein (LPS) or an LPS and SCFA cocktail. Scale bars: 50 μm. G, Diameter of myotubes among the three groups described in (F). H, I, Alternations of Atrogin-1 and MuRF1 mRNA expression in C2C12 myotubes treated with LPS and/or SCFA cocktail. J-L, Alternations of PGC1α, Tfam, and CPT1b mRNA expression in C2C12 myotubes treated with LPS and/or SCFA cocktail. H-L, data derived from $n = 4$ per group. Data are shown as means \pm SEM. * $p < 0.05$, ** $p < 0.01$, *** $p < 0.001$. FF, fiber-free; FR, fiber-rich

obesity and metabolic diseases, where systemic inflammation caused by enhanced gut mucosa permeability and subsequent endotoxemia is considered to be a causative factor of disease development.^{33,35,36} At a lower taxonomic level, we observed the significant recovery of unclassified *S24-7 family*, *Bifidobacterium*, and *Akkermansia* by PHGG supplementation in C26 mice, which may explain the decreased diversity in microbial abundance and evenness in this group. *S24-7*, which was a predominant member of the gut microbiota in the C26-FR group, has been reported to possess fermentative pathways for producing succinate, acetate, and propionate.³⁷ We assume that this bacterium largely contributed to the preservation of fecal SCFAs. Of note, *Bifidobacterium* has been reported to restore the reduced intestinal mucus layer caused by consumption of a low-fiber Western diet.³² Moreover, *Akkermansia muciniphila* has also been reported regarding its importance in improving the gut barrier function and reducing endotoxemia.³⁸ However, the detailed mechanisms underlying the

effects of these bacteria on the host are still unclear, especially in the area of cancer cachexia; thus, further research is warranted.

The host's immunological system responds to the tumor by producing proinflammatory cytokines including IL-1β, IL-6, TNF-α, and INF-γ.^{3,7} These cytokines are essential for driving inflammatory reactions needed to overcome the tumor burden, while also playing a critical role in muscle wasting by directly targeting muscle tissue. IL-6 is widely known as a key mediator of cancer cachexia, as these inhibitors were reported to markedly prevent cancer-associated muscle wasting in previous studies.^{39,40} In our study, IL-6, but not other proinflammatory cytokines such as IL-1β, TNF-α, and INF-γ, was involved in the development of C26-induced cachexia, and the marked suppression of IL-6 in C26 mice fed a high-fiber diet was associated with a preserved muscle mass. Notably, IL-6 was significantly positively correlated with LBP, supporting the relevance of increased gut permeability in cancer-induced muscle loss. Other cytokines including IL-5, IL12(p70), G-CSF, GM-CSF, and MIP-1a and b,

which showed decreased levels in tumor-bearing mice, may have had some influence, although little is known regarding their contribution to cachexia.

Previous studies indicated that SCFAs, major microbial metabolites, can strengthen the gut barrier by promoting mucus production and secretion.^{41,42} Furthermore, these metabolites may be partially involved in the metabolism and function of skeletal muscle through modification of mitochondrial activity.^{20,43} In light of these reports, while the role of SCFAs in the context of cancer cachexia has yet to be elucidated, beneficial effects are expected. Our data revealed that fecal SCFA levels were relatively low in cachectic mice, although the reduction was mitigated when PHGG supplementation was given. Indeed, this could be another explanation for the retention of the mucus layer. Markers related to mitochondria were not fully affected in our mouse model, although we did examine the possible protective effect of SCFAs on muscle atrophy by *in vitro* methods. However, it should be noted as a limitation that the concentrations of LPS and SCFAs set in the *in vitro* experiment were higher than that in the circulating system.^{11,44} Taken together, our findings suggest that SCFAs may be involved in preventing cancer-induced muscle wasting, although further investigation is warranted.

In conclusion, our observations suggest that dietary fiber alters the gut microbiota and restores the gut barrier function in cachectic mice and that these modifications induce a systemic anti-inflammatory effect, thereby attenuating muscle wasting. Among the complex mechanisms of cancer-induced muscle atrophy, cross-talk between the gut environment and skeletal muscle may be at least partially involved. Although further research is required in this underexplored area, the novel insights obtained in this study may indicate a potential nutritional strategy against cancer cachexia.

ACKNOWLEDGMENTS

This work was partly supported by MAFF Commissioned project study on "Project for the realization of foods and dietary habits to extend healthy life expectancy" (Grant Number JPJ009842). This work was also supported by JSPS KAKENHI (Grant Number JP 20K07787).

DISCLOSURE

Yuji Naito received scholarship funds from Taiyo Kagaku Co., Ltd. and from EA Pharma Co. Ltd.; a collaboration research fund from Taiyo Kagaku Co., Ltd.; and lecture fees from Mylan EPD Co., Takeda Pharma. Co. Ltd., Mochida Pharma. Co. Ltd., EA Pharma. Co. Ltd., Otsuka Pharma. Co. Ltd., and Miyarisan Pharma. Co. Ltd. The present research was partly supported by these funds. Neither the funding agency nor any outside organization has participated in the study design or has any competing interests. These companies have approved the final version of the manuscript. The other authors have no conflict of interest to declare.

ETHICAL APPROVAL

All animals were maintained and experimental procedures were carried out following National Institutes of Health (NIH) guidelines for the use of experimental animals. All experimental protocols were

approved by the Animal Care Committee of the Kyoto Prefectural University of Medicine (No.M2021-538).

DATA AVAILABILITY STATEMENT

The raw microarray data generated in this study are available in ArrayExpress under accession number E-MTAB-11094. Sequence data used in this study have been submitted to Sequence Read Archive (SRA) with the accession number PRJNA772926 (available from 31st/Jan/2022). Other data that support the findings of this study are available on reasonable request from the corresponding author.

ORCID

Tomoki Sakakida  <https://orcid.org/0000-0003-1913-7923>

Takeshi Ishikawa  <https://orcid.org/0000-0002-5770-9710>

Yuki Endo  <https://orcid.org/0000-0002-8017-1744>

REFERENCES

- Tisdale MJ. Cachexia in cancer patients. *Nat Rev Cancer*. 2002;2(11):862-871.
- Argilés JM. The 2015 ESPEN Sir David Cuthbertson lecture: inflammation as the driving force of muscle wasting in cancer. *Clin Nutr*. 2017;36(3):798-803.
- Argilés JM, Busquets S, Stemmler B, López-Soriano FJ. Cancer cachexia: understanding the molecular basis. *Nat Rev Cancer*. 2014;14(11):754-762.
- Bodine SC, Latres E, Baumhueter S, et al. Identification of ubiquitin ligases required for skeletal muscle atrophy. *Science*. 2001;294(5547):1704-1708.
- Gomes MD, Lecker SH, Jagoe RT, Navon A, Goldberg AL. Atrogin-1, a muscle-specific F-box protein highly expressed during muscle atrophy. *Proc Natl Acad Sci USA*. 2001;98(25):14440-14445.
- Porporato PE. Understanding cachexia as a cancer metabolism syndrome. *Oncogenesis*. 2016;5(2):e200.
- Tisdale MJ. Mechanisms of cancer cachexia. *Physiol Rev*. 2009;89(2):381-410.
- Suh SY, Choi YS, Yeom CH, et al. Interleukin-6 but not tumour necrosis factor- α predicts survival in patients with advanced cancer. *Support Care Cancer*. 2013;21(11):3071-3077.
- Ticinesi A, Lauretani F, Milani C, et al. Aging gut microbiota at the cross-road between nutrition, physical frailty, and sarcopenia: is there a gut-muscle axis? *Nutrients*. 2017;9(12):1303.
- Sovran B, Hugenholtz F, Elderman M, et al. Age-associated impairment of the mucus barrier function is associated with profound changes in microbiota and immunity. *Sci Rep*. 2019;9(1):1437.
- Puppa MJ, White JP, Sato S, Cairns M, Baynes JW, Carson JA. Gut barrier dysfunction in the Apc(Min/+) mouse model of colon cancer cachexia. *Biochim Biophys Acta*. 2011;1812(12):1601-1606.
- Bindels LB, Neyrinck AM, Loumaye A, et al. Increased gut permeability in cancer cachexia: mechanisms and clinical relevance. *Oncotarget*. 2018;9(26):18224-18238.
- Bindels LB, Neyrinck AM, Salazar N, et al. Non digestible oligosaccharides modulate the gut microbiota to control the development of leukemia and associated cachexia in mice. *PLoS One*. 2015;10(6):e0131009.
- Wijler LA, Raats DAE, Elias SG, et al. Specialized nutrition improves muscle function and physical activity without affecting chemotherapy efficacy in C26 tumour-bearing mice. *J Cachexia Sarcopenia Muscle*. 2021;12(3):796-810.
- Varian BJ, Gourishetti S, Poutahidis T, et al. Beneficial bacteria inhibit cachexia. *Oncotarget*. 2016;7(11):11803-11816.

16. El Kaoutari A, Armougoum F, Gordon JI, Raoult D, Henrissat B. The abundance and variety of carbohydrate-active enzymes in the human gut microbiota. *Nat Rev Microbiol*. 2013;11(7):497-504.
17. Gao Z, Yin J, Zhang J, et al. Butyrate improves insulin sensitivity and increases energy expenditure in mice. *Diabetes*. 2009;58(7):1509-1517.
18. Walsh ME, Bhattacharya A, Sataranatarajan K, et al. The histone deacetylase inhibitor butyrate improves metabolism and reduces muscle atrophy during aging. *Aging Cell*. 2015;14(6):957-970.
19. Ohashi Y, Sumitani K, Tokunaga M, Ishihara N, Okubo T, Fujisawa T. Consumption of partially hydrolysed guar gum stimulates Bifidobacteria and butyrate-producing bacteria in the human large intestine. *Benef Microbes*. 2015;6(4):451-455.
20. Lahiri S, Kim H, Garcia-Perez I, et al. The gut microbiota influences skeletal muscle mass and function in mice. *Sci Transl Med*. 2019;11(502):eaa5662.
21. Ono Y, Maejima Y, Saito M, et al. TAK-242, a specific inhibitor of Toll-like receptor 4 signalling, prevents endotoxemia-induced skeletal muscle wasting in mice. *Sci Rep*. 2020;10(1):694.
22. Matsuyama T, Ishikawa T, Okayama T, et al. Tumor inoculation site affects the development of cancer cachexia and muscle wasting. *Int J Cancer*. 2015;137(11):2558-2565.
23. da Huang W, Sherman BT, Lempicki RA. Systematic and integrative analysis of large gene lists using DAVID bioinformatics resources. *Nat Protoc*. 2009;4(1):44-57.
24. Desai MS, Seekatz AM, Koropatkin NM, et al. A Dietary fiber-deprived gut microbiota degrades the colonic mucus barrier and enhances pathogen susceptibility. *Cell*. 2016;167(5):1339-53 e21.
25. Higashimura Y, Baba Y, Inoue R, et al. Agaro-oligosaccharides regulate gut microbiota and adipose tissue accumulation in mice. *J Nutr Sci Vitaminol (Tokyo)*. 2017;63(4):269-276.
26. Janssen S, McDonald D, Gonzalez A, et al. Phylogenetic placement of exact amplicon sequences improves associations with clinical information. *mSystems*. 2018;3(3):e00021-18.
27. Ushida K, Sakata T. Effect of pH on oligosaccharide fermentation by porcine cecal digesta. *Anim Sci J*. 1998;69:100-107.
28. Milan G, Romanello V, Pescatore F, et al. Regulation of autophagy and the ubiquitin-proteasome system by the FoxO transcriptional network during muscle atrophy. *Nat Commun*. 2015;6:6670.
29. Schumann RR. Old and new findings on lipopolysaccharide-binding protein: a soluble pattern-recognition molecule. *Biochem Soc Trans*. 2011;39(4):989-993.
30. Roberts EW, Deonarine A, Jones JO, et al. Depletion of stromal cells expressing fibroblast activation protein- α from skeletal muscle and bone marrow results in cachexia and anemia. *J Exp Med*. 2013;210(6):1137-1151.
31. Cani PD, Possemiers S, Van de Wiele T, et al. Changes in gut microbiota control inflammation in obese mice through a mechanism involving GLP-2-driven improvement of gut permeability. *Gut*. 2009;58(8):1091-1103.
32. Schroeder BO, Birchenough GMH, Stahlman M, et al. Bifidobacteria or fiber protects against diet-induced microbiota-mediated colonic mucus deterioration. *Cell Host Microbe*. 2018;23(1):27-40 e7.
33. Zou J, Chassaing B, Singh V, et al. Fiber-mediated nourishment of gut microbiota protects against diet-induced obesity by restoring IL-22-mediated colonic health. *Cell Host Microbe*. 2018;23(1):41-53. e4.
34. González-Sarrías A, Núñez-Sánchez MA, Ávila-Gálvez MA, et al. Consumption of pomegranate decreases plasma lipopolysaccharide-binding protein levels, a marker of metabolic endotoxemia, in patients with newly diagnosed colorectal cancer: a randomized controlled clinical trial. *Food Funct*. 2018;9(5):2617-2622.
35. Cani PD, Bibiloni R, Knauf C, et al. Changes in gut microbiota control metabolic endotoxemia-induced inflammation in high-fat diet-induced obesity and diabetes in mice. *Diabetes*. 2008;57(6):1470-1481.
36. Jakobsson HE, Rodríguez-Piñero AM, Schütte A, et al. The composition of the gut microbiota shapes the colon mucus barrier. *EMBO Rep*. 2015;16(2):164-177.
37. Ormerod KL, Wood DL, Lachner N, et al. Genomic characterization of the uncultured Bacteroidales family S24-7 inhabiting the guts of homeothermic animals. *Microbiome*. 2016;4(1):36.
38. Everard A, Belzer C, Geurts L, et al. Cross-talk between Akkermansia muciniphila and intestinal epithelium controls diet-induced obesity. *Proc Natl Acad Sci U S A*. 2013;110(22):9066-9071.
39. Zaki MH, Nemeth JA, Trikha M. CNTO 328, a monoclonal antibody to IL-6, inhibits human tumor-induced cachexia in nude mice. *Int J Cancer*. 2004;111(4):592-595.
40. Fujita J, Tsujinaka T, Yano M, et al. Anti-interleukin-6 receptor antibody prevents muscle atrophy in colon-26 adenocarcinoma-bearing mice with modulation of lysosomal and ATP-ubiquitin-dependent proteolytic pathways. *Int J Cancer*. 1996;68(5):637-643.
41. Barcelo A, Claustre J, Moro F, Chayvialle JA, Cuber JC, Plaisancié P. Mucin secretion is modulated by luminal factors in the isolated vascularly perfused rat colon. *Gut*. 2000;46(2):218-224.
42. Wells JM, Brummer RJ, Derrien M, et al. Homeostasis of the gut barrier and potential biomarkers. *Am J Physiol Gastrointest Liver Physiol*. 2017;312(3):G171-G193.
43. Frampton J, Murphy KG, Frost G, Chambers ES. Short-chain fatty acids as potential regulators of skeletal muscle metabolism and function. *Nat Metab*. 2020;2(9):840-848.
44. Bloemen JG, Venema K, van de Poll MC, Olde Damink SW, Buurman WA, Dejong CH. Short chain fatty acids exchange across the gut and liver in humans measured at surgery. *Clin Nutr*. 2009;28(6):657-661.

SUPPORTING INFORMATION

Additional supporting information may be found in the online version of the article at the publisher's website.

How to cite this article: Sakakida T, Ishikawa T, Doi T, et al. Water-soluble dietary fiber alleviates cancer-induced muscle wasting through changes in gut microenvironment in mice. *Cancer Sci*. 2022;113:1789-1800. doi:[10.1111/cas.15306](https://doi.org/10.1111/cas.15306)